Supporting Information

3D Printing of Living Responsive Materials and Devices

*Xinyue Liu, Hyunwoo Yuk, Shaoting Lin, German Alberto Parada, Tzu-Chieh Tang, Eléonore Tham, Cesar de la Fuente-Nunez, Timothy K. Lu, Xuanhe Zhao**

X. Liu, H. Yuk, S. Lin, G. A. Parada, Prof. X. Zhao
Soft Active Materials Laboratory, Department of Mechanical Engineering, Massachusetts Institute of Technology, Cambridge, MA 02139, USA
E-mail: zhaox@mit.edu
G. A. Parada
Department of Chemical Engineering, Massachusetts Institute of Technology, Cambridge, MA 02139, USA
T. Tang, E. Tham, C. Fuente-Nunez, Prof. T. K. Lu
Synthetic Biology Group, Research Laboratory of Electronics, Massachusetts Institute of Technology, Cambridge, MA 02139, USA
T. Tang, C. Fuente-Nunez, Prof. T. K. Lu
Department of Biological Engineering, Massachusetts Institute of Technology, Cambridge, MA 02139, USA
E. Tham
Department of Materials Science and Engineering, Massachusetts Institute of Technology, Cambridge, MA 02139, USA
Dr. C. Fuente-Nunez, Prof. T. K. Lu
Department of Electrical Engineering and Computer Science, Massachusetts Institute of Technology, Cambridge, MA 02139, USA
Prof. X. Zhao
Department of Civil and Environmental Engineering, Massachusetts Institute of Technology, Cambridge, MA 02139, USA

Development of the model for living materials

Quantifying the operation of 3D printed living materials requires a general model that accounts for the transportations of chemicals and the responses of cells in the materials[1-3]. The chemical diffusion in the hydrogel matrices is taken to follow the Fick's law[2]

$$\frac{\partial C}{\partial t} = -D\nabla C \tag{1}$$

where C is the moles of the signaling chemicals per unit volume of hydrogel (i.e., chemical concentration), t is the current time, and D is the diffusion coefficient of the chemical in hydrogel. The biochemical reactions in cells depend on the genetic circuits of different cell types. For the inducible GFP expression in cells, we adopt the induction model in previous works, which considers the processes of immature protein synthesis, protein maturation, cell division, and protein degradation[2, 4]. We denote the numbers of immature protein and mature protein in a cell as n and f, respectively, and the numbers of cell per unit volume (i.e., cell density) in the hydrogel as N. Their rates of variation can be expressed as[2, 3]

$$\frac{\partial n}{\partial t} = P_m \cdot \frac{C^h}{C^h + K^h} - m \cdot n - \mu \cdot (1 - \frac{N}{N_m}) \cdot n - k \cdot n \tag{2}$$

$$\frac{\partial f}{\partial t} = m \cdot n - \mu \cdot (1 - \frac{N}{N_m}) \cdot f - k \cdot f \tag{3}$$

$$\frac{\partial N}{\partial t} = \mu \cdot (1 - \frac{N}{N_m}) \cdot N \tag{4}$$

where P_m is the maximum rate of immature GFP expression, h is the Hill coefficient, K is the half-maximal parameter, m is the maturation constant, μ is the cell growth constant, N_m is the maximum cell density in hydrogel, and k is the degradation constant. Note that the measurable fluorescence intensity in the hydrogel is the number of fluorescent protein per unit of volume in hydrogel, that is $N \cdot f$.

Table S1. Input and output chemicals or cells for logic gate construction.

Gate	Input a	Input b	Output
Buffer	AHL (100 nM)	/	AHL/GFP+ cells
NOT	AHL (100 nM)	/	AHL/GFP- cells
AND	aTc (200 ng/mL)	aTc/AHL+ cells	AHL/GFP+ cells
OR	AHL (100 nM)	Rham (12 mM)	AHL/GFP+ cells Rham/GFP+ cells
NAND	aTc (200 ng/mL)	aTc/AHL+ cell	AHL/GFP- cells

Table S2. Parameter values for the spatiotemporal model in Fig. 4. These values are adopted from our previous paper[2].

Parameter	Definition	Value
D	diffusion coefficient of the chemical in hydrogel	2.0×10^{-10} m^2/s
C_0	initial chemical concentration in hydrogel with chemical	200 nM
P_m	maximum rate of immature GFP expression	1000 s^{-1}
h	Hill coefficient	1.66
K	half-maximal parameter	1.5 nM
m	maturation constant	1.16×10^{-3} s^{-1}
μ	cell growth constant	1.20×10^{-4} s^{-1}
N_m	maximum cell density in hydrogel	3.5×10^{8} cells/ml
k	degradation constant	2.0×10^{-5} s^{-1}
n_0	initial immature protein in a cell	0
f_0	initial mature protein in a cell	0
N_0	initial cell density in hydrogel	1.6×10^{8} cells/ml

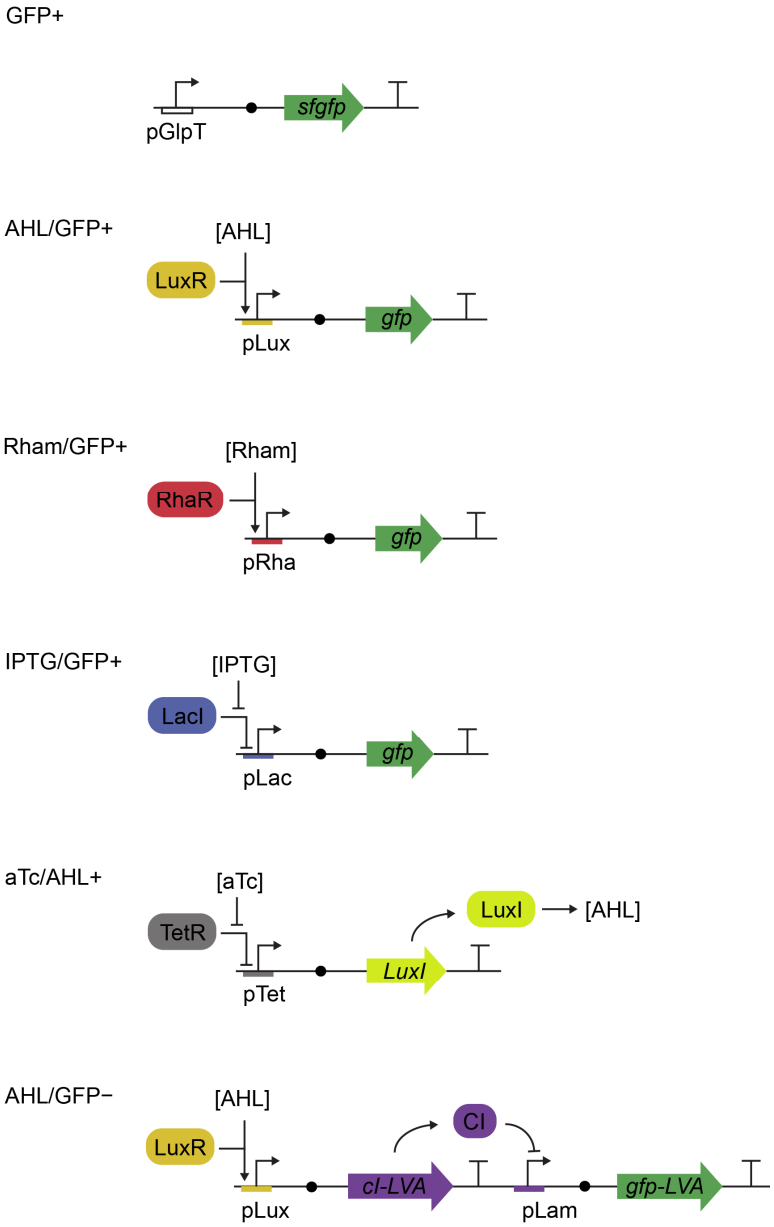

Figure S1. Circuit diagrams of the engineered bacterial strains. The inducers (such as AHL, Rham, IPTG, and aTc) interact with transcriptional factors (such as, LuxR, RhaR, LacI, and TetR, respectively), and induce downstream gene expression. pGlpT is a constitutive promoter. cI/pLam repressor module acts as a invertor for GFP expression in the cell. *sfgfp* denotes a gene for superfolder GFP. *LVA* denotes a gene for protein degradation tag, which reduce the GFP half-life from two days to two hours.

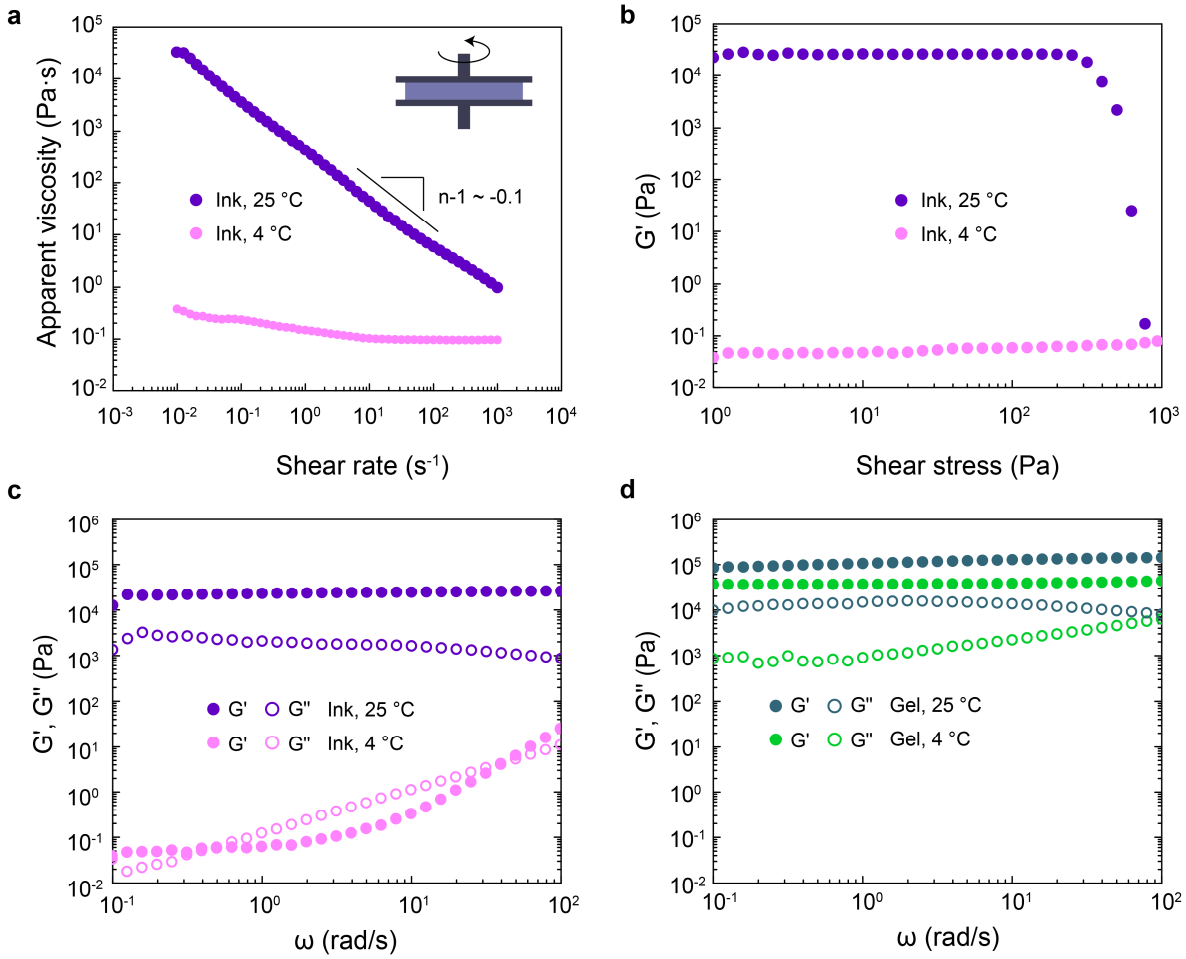

Figure S2. Rheological behavior of Pluronic F127-DA ink and UV-crosslinked hydrogel. a) Ink apparent viscosity as a function of shear rate at 25°C and 4°C. b) Ink shear storage moduli (G') as a function of shear stress at 25°C and 4°C, measured in oscillatory mode at 1 Hz. c) Ink shear storage moduli (G', solid dots) and loss moduli (G", open dots) as a function of angular velocity (ω) at 25°C and 4°C. d) UV crosslinked hydrogel shear storage moduli (G', solid dots) and loss moduli (G", open dots) as a function of angular velocity (ω) at 25°C and 4°C.

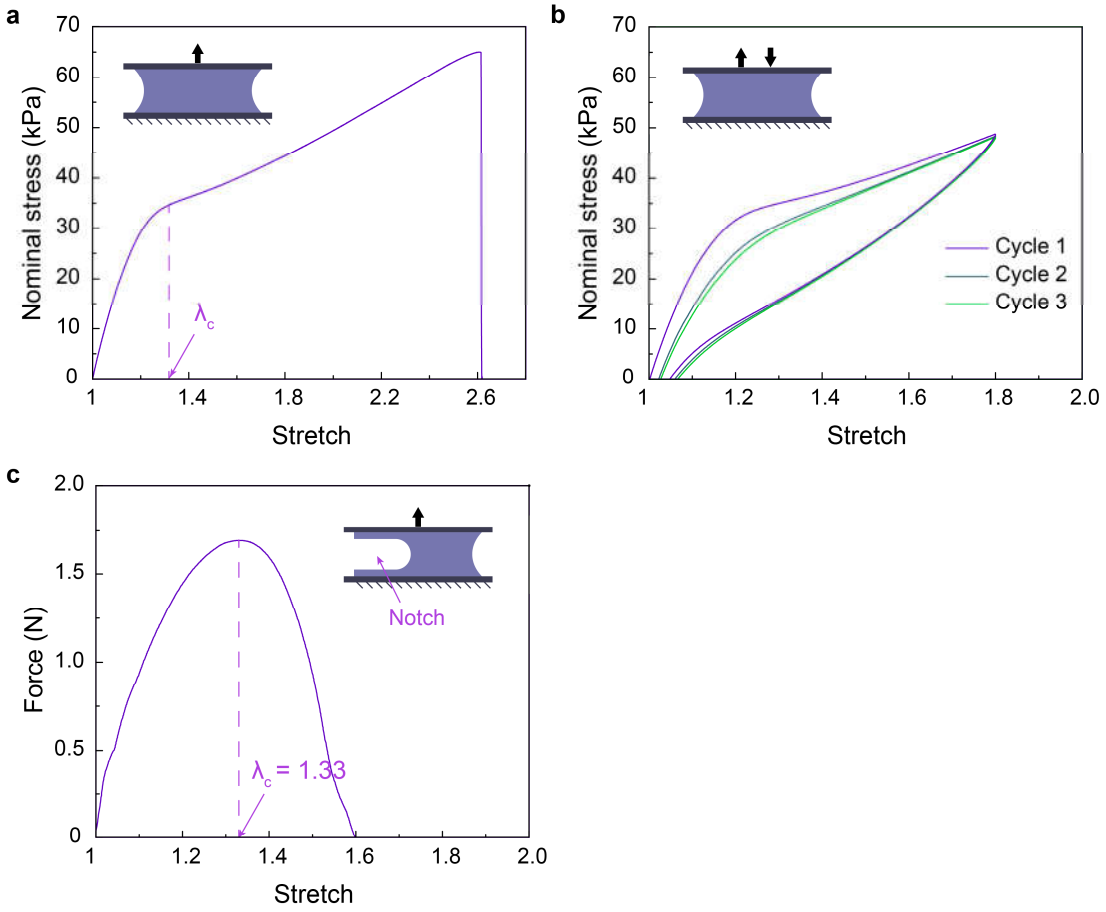

Figure S3. Mechanical behavior of Pluronic F127-DA UV-crosslinked hydrogel. a) Stress–stretch curve of the hydrogel. b) Cyclic stress-stretch curve measured by loading and unloading the hydrogel to a stretch of 1.8. Three cycles are carried out. c) Stress–stretch curve of the notched hydrogel. The critical stretch for steady crack propagation measured in notched samples is indicated as λ_c.

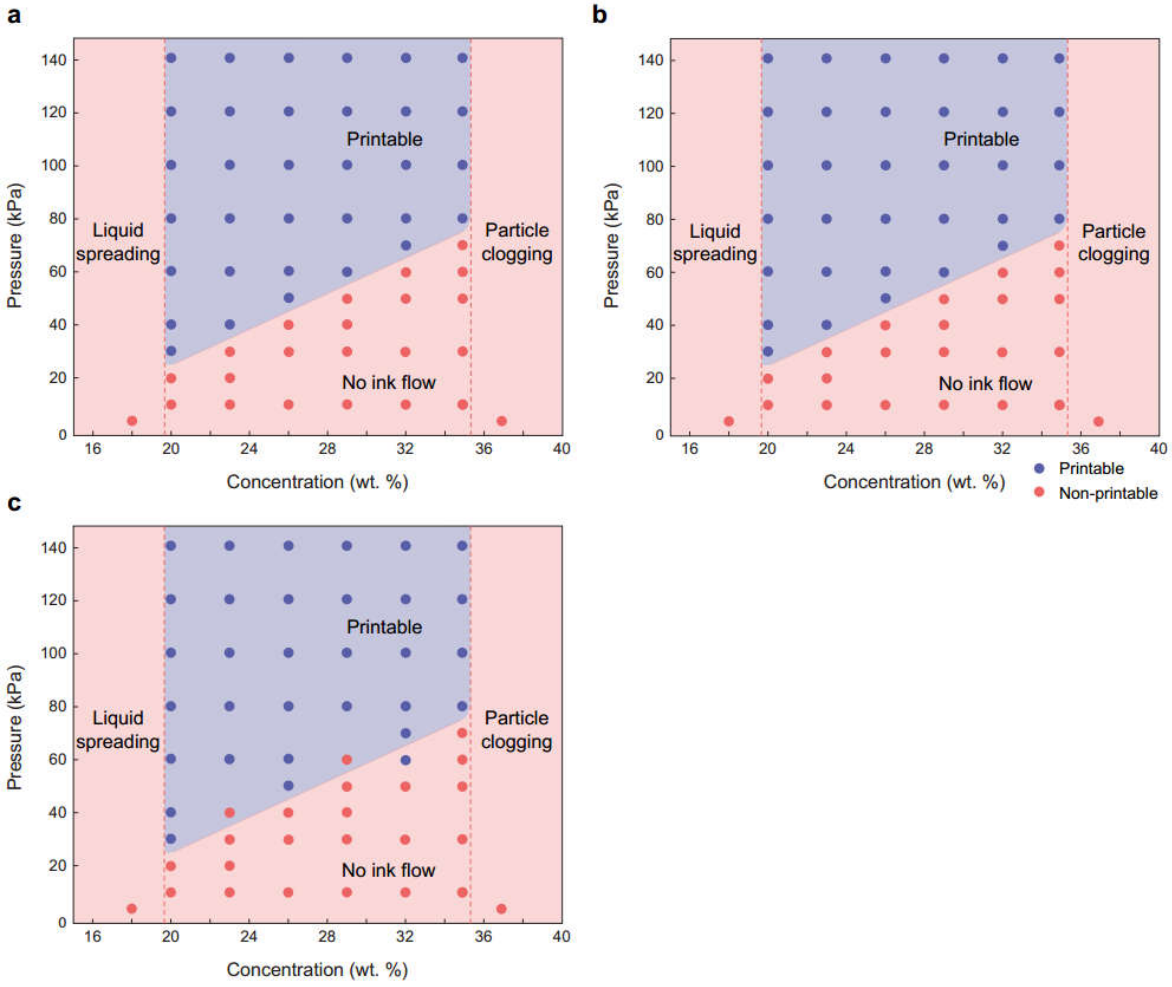

Figure S4. Printability diagrams with different nozzle dimensions. a-c) Phase diagrams for Pluronic F127-DA ink printability, which contains non-printable (red) and printable (blue) regions. The tests are carried out with 200 μm (a),100 μm (b), and 30 μm (c) in nozzle size.

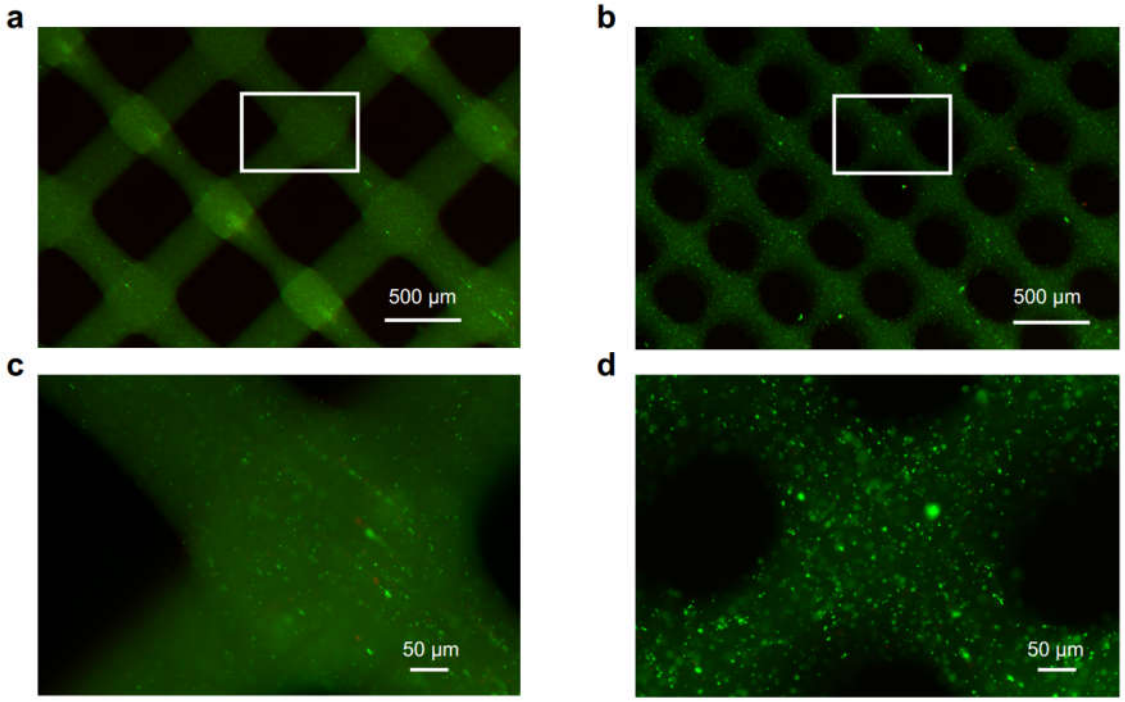

Figure S5. Cell viability in Pluronic F127-DA UV-crosslinked hydrogel tested by live-dead assay 24 h after printing. a,c) Fluorescent images of bacterial cells in printed living materials with 200 µm feature size. b,d) Fluorescent images of bacterial cells in printed living materials with 100 µm feature size. Red denotes dead cells (resulting from increased uptake of propidium iodide into membrane damaged/dead cells), while green denotes live cells. Scale bars are shown in images.

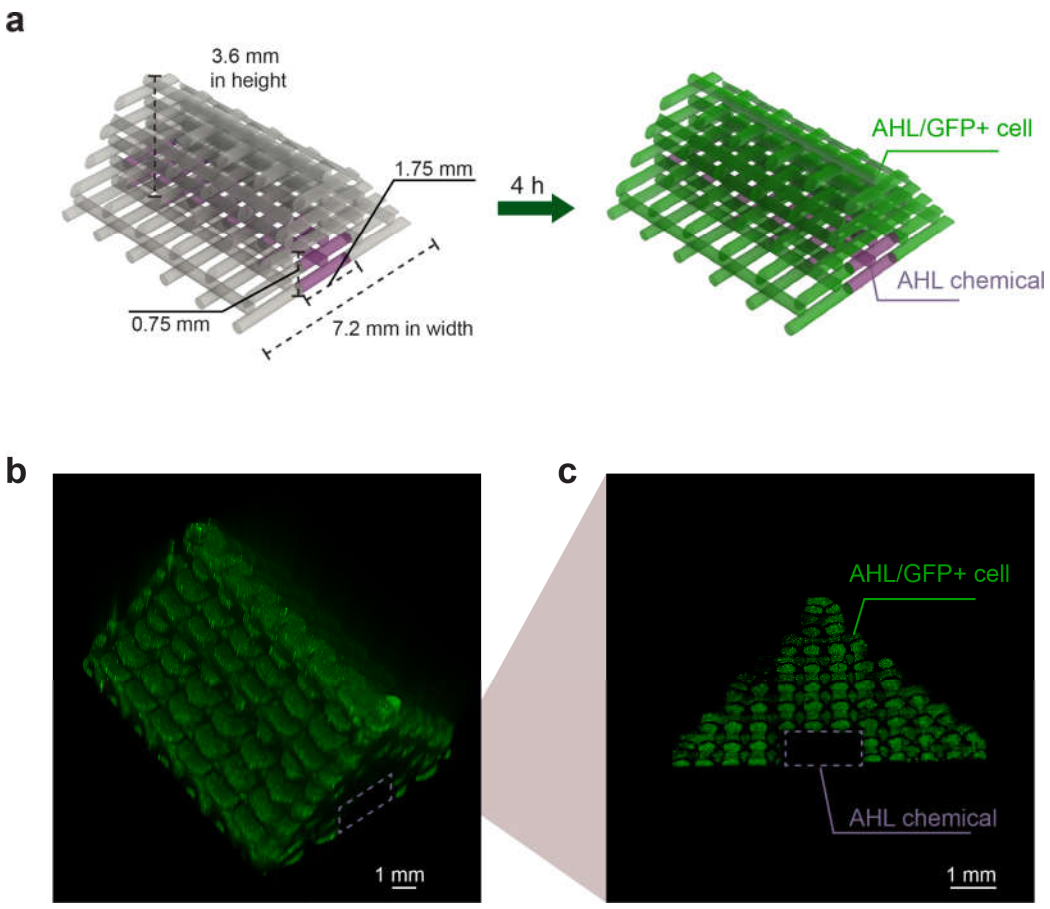

Figure S6. 3D patterning of a living structure. a) Schematic illustration of a 3D living structure (3.6 mm in height). The hydrogel inks contain AHL and AHL/GFP+ cell in different regions of the 3D structure. Once the cells are induced (~4 hours after printing), the hydrogel region with cells in the living structure become fluorescent. b) 3D reconstructed fluorescent images and c) cross-section fluorescent images of a the 3D living structure with 18 layers of hydrogel deposition. Scale bar in b-c, 1mm.

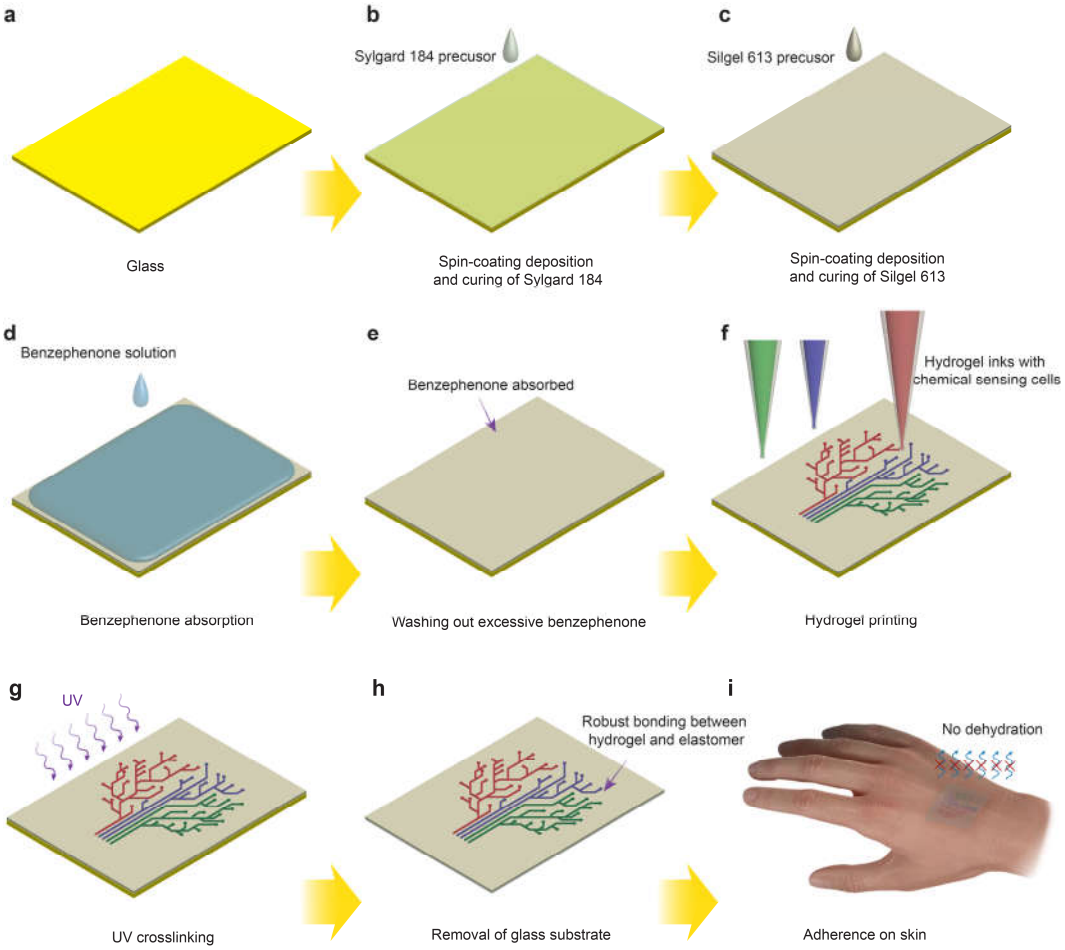

Figure S7. Schematic illustration of living tattoo fabrication. a-c) Spin-coating and curing of two types of elastomeric thin films on glass substrate. d,e) Surface activation of elastomer by benzophenone solution. f) Printing of hydrogel inks containing bacterial cells on the elastomer. g) Hydrogel crosslinking and surface bonding by UV irradiation. h) Removal of the glass substrate. i) adherence of the living tattoo to skin.

SUPPLEMENTARY MOVIE CAPTIONS

Video S1: The multimaterial direct ink writing process (speed × 16) of a living material with a 3D structure.

Video S2: The multimaterial direct ink writing process (speed × 4) of a living material with a 2D tree-like pattern.

Video S3: Spatiotemporal responses of a living material with the 2D tree-like pattern over three hours.

References

[1] A. M. Tayar, E. Karzbrun, V. Noireaux, R. H. Bar-Ziv, *Nature Physics* **2015**, *11*, 1037.
[2] X. Liu, T.-C. Tang, E. Tham, H. Yuk, S. Lin, T. K. Lu, X. Zhao, *Proc. Natl. Acad. Sci. USA* **2017**, *114*, 2200.
[3] G. E. Dilanji, J. B. Langebrake, P. De Leenheer, S. J. Hagen, *Journal of the American Chemical Society* **2012**, *134*, 5618.
[4] J. H. Leveau, S. E. Lindow, *Journal of bacteriology* **2001**, *183*, 6752.